

# In vivo anomalous diffusion and weak ergodicity breaking of lipid granules

Jae-Hyung Jeon,<sup>1</sup> Vincent Tejedor,<sup>2</sup> Stas Burov,<sup>3</sup> Eli Barkai,<sup>3</sup> Christine Selhuber-Unkel,<sup>4,5</sup> Kirstine Berg-Sørensen,<sup>6</sup> Lene Oddershede,<sup>4</sup> and Ralf Metzler<sup>1</sup>

<sup>1</sup>Physics Department T30g, Technical University of Munich, 85747 Garching, Germany

<sup>2</sup>Physique Théorique de la matière condensée, Université Pierre et Marie Curie, 4 place Jussieu, 75252 Paris, France

<sup>3</sup>Physics Department, Bar-Ilan University, Ramat Gan 52900, Israel

<sup>4</sup>Niels Bohr Institute, Blegdamsvej 17, 2100 København Ø, Denmark

<sup>5</sup>Institute for Materials Science, University of Kiel, Kaiserstraße 2, 24143 Kiel, Germany

<sup>6</sup>Physics Department, Technical University of Denmark, 2800 Kongens Lyngby, Denmark

(Dated: 22nd October 2018)

Combining extensive single particle tracking microscopy data of endogenous lipid granules in living fission yeast cells with analytical results we show evidence for anomalous diffusion and weak ergodicity breaking. Namely we demonstrate that at short times the granules perform subdiffusion according to the laws of continuous time random walk theory. The associated violation of ergodicity leads to a characteristic turnover between two scaling regimes of the time averaged mean squared displacement. At longer times the granule motion is consistent with fractional Brownian motion.

PACS numbers: 87.16.dj,87.10.Mn,05.40.-a,02.50.-r

Crowded colloidal systems of hard and soft core particles display a rich physical behavior including dynamic arrest, non-exponential relaxation, and anomalous diffusion [1]. In biological cells the cytoplasm is a crowded soft core colloid made up of large biopolymers such as ribosomes, proteins, or RNA, occupying volume fractions of 34% or above [2, 3], amidst small particles such as water, ions, and lower mass fraction biopolymers. Such crowding significantly impacts cellular biochemical reactions [2] and effects subdiffusion of the form [4, 5]

$$\langle \mathbf{r}^2(t) \rangle \propto K_\alpha t^\alpha, \quad 0 < \alpha < 1, \quad (1)$$

of larger molecules or tracers in living cells [3, 6–16]. While normal diffusion, by virtue of the central limit theorem, is characterized by the universal Gaussian probability density function and therefore uniquely determined by the first and second moments [17], anomalous diffusion of the form (1) is non-universal and may be caused by different stochastic mechanisms. These would give rise to vastly different behavior for diffusional mixing, diffusion-limited reactions, signaling, or regulatory processes. To better understand cellular dynamics, knowledge of the underlying stochastic mechanism is thus imperative.

Here we report experimental evidence from extensive single trajectory time series of lipid granule motion in *Schizosaccharomyces pombe* (*S. pombe*) fission yeast cells obtained from tracking with optical tweezers (resolving  $10^{-6}$  sec to 1 sec) and video microscopy ( $10^{-2}$  sec to 100 sec). Using complementary analysis tools we demonstrate that at short times the data are described best by continuous time random walk (CTRW) subdiffusion, revealing pronounced features of weak ergodicity breaking in the time averaged mean squared displacement. At longer times the stochastic mechanism is closest to subdiffusive fractional Brownian motion (FBM). The time scales over which this anomalous behavior persists is rel-

evant for biological processes occurring in the cell. Anomalous diffusion may indeed be a good strategy for cellular signaling and reactions [7, 8].

CTRW and FBM both effect anomalous diffusion of the type (1) [18]. Subdiffusive CTRWs are random walks with finite variance  $\langle \delta x^2 \rangle$  of jump lengths, while the waiting times between successive jumps are drawn from a density  $\psi(t) \simeq \tau^\alpha / t^{1+\alpha}$  with diverging characteristic time [4, 17]. Such scale-free behavior results from multiple trapping events in, e.g., comb-like structures [19] or random energy landscapes [20]. Power-law waiting time distributions were also identified for tracer motion in reconstituted actin networks [21]. Subdiffusive FBM is a random process driven by Gaussian noise  $\xi$  with long-range correlations,  $\langle \xi(0)\xi(t) \rangle \simeq \alpha(\alpha-1)t^{\alpha-2}$  [22], and it is related to fractional Langevin equations [23]. The finite characteristic time scales associated with FBM contrast the ageing property of the subdiffusive CTRW processes [Supplementary Material (SM)].

Single particle tracking microscopy has become a standard tool to probe the motion of individual tracers, especially inside living cells, and provides valuable insights into cellular dynamics [6]. The recorded time series  $\mathbf{r}(t)$  are analyzed in terms of the time averaged mean squared displacement as function of the lag time  $\Delta$ ,

$$\overline{\delta^2(\Delta, T)} = \frac{1}{T-\Delta} \int_0^{T-\Delta} [\mathbf{r}(t+\Delta) - \mathbf{r}(t)]^2 dt, \quad (2)$$

where  $T$  is the total measurement time. CTRW and FBM subdiffusion show markedly different behavior of  $\overline{\delta^2(\Delta, T)}$  [24–27]. Subdiffusion of the form  $\overline{\delta^2} \simeq \Delta^\alpha$  was found in several tracking experiments *in vivo* [8–14]. Crowding-induced subdiffusion was also observed in controlled environments, e.g., in concentrated protein and dextran solutions [16, 28–30]. While FBM was proposed as stochastic mechanism in some of these systems

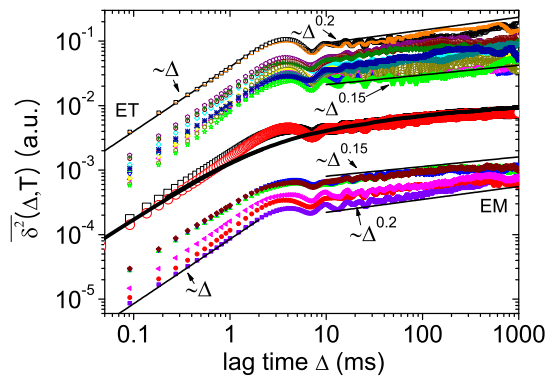


Figure 1: Time averaged mean squared displacement  $\overline{\delta^2}$  from individual trajectories of lipid granules in *S.pombe* in Early Mitotic cells (lower curves) and in Early Telophase (upper curves), measured by optical tweezers [33]. A distinct turnover from  $\overline{\delta^2} \simeq \Delta$  to  $\simeq \Delta^\beta$  ( $\beta \approx 0.10 \dots 0.20$ ) occurs. The two thick lines in the middle show the averages of the ET (red  $\circ$ ) and EM (black  $\square$ ) data sets. The overlaid thick black line is the result of CTRW simulations in an harmonic potential. ET versus EM curves are shifted vertically.

[14, 16, 31] CTRW subdiffusion has not yet been identified. Here we demonstrate that the short time motion of lipid granules in *S.pombe* cells follows the laws of CTRW subdiffusion and features weak ergodicity breaking.

*Short time behavior.* Granule motion was recorded in an optical tweezers setup (SM). In the experiment the trap is initially centered onto the granule such that no force is exerted. When the granule starts to move away from the trap center it experiences a restoring Hookean force [32]. The measured  $\overline{\delta^2}(\Delta)$  curves from two different cell stages are shown in Fig. 1 [33], along with a typical sample trajectory in Fig. 5a (SM). In Fig. 1 a distinct turnover is observed from an initial linear growth  $\overline{\delta^2} \simeq \Delta$  to a power-law behavior  $\overline{\delta^2} \simeq \Delta^\beta$  with  $\beta \approx 0.15 \dots 0.20$ .

The size of the lipid granules is about 300 nm. In addition to the amplitude scatter between different trajectories expected from CTRW theory [24, 26], the fluctuations of the data in Fig. 1 are due to natural granule size variations and different optical conditions for each trajectory. We note that oscillations around the turnover may arise for subdiffusion in an underdamped medium [34].

Evaluating extensive data for the granule motion analogous to the data presented here by *ensemble* averages, anomalous diffusion with  $\alpha \approx 0.80 \dots 0.85$  yields in a range of 0.1 to 3 msec [13]. In contrast, in Fig. 1 the initial behavior of  $\overline{\delta^2}$  corresponding to this time range does not exhibit any apparent anomaly but scales like  $\overline{\delta^2} \simeq \Delta^1$ . At longer lag time  $\Delta$  due to the trap force one would expect  $\overline{\delta^2}$  to saturate to a stationary thermal value; instead, the regime  $\overline{\delta^2} \simeq \Delta^\beta$  appears. This behavior is consistently observed in different cell stages (Fig. 1).

Such a peculiar behavior is fully consistent with CTRW subdiffusion: For free motion one finds  $\overline{\delta^2} \simeq \Delta/T^{1-\alpha}$ , whose  $\Delta$  scaling is independent of  $\alpha$ , while the corresponding ensemble average follows Eq. (1) [24, 25]. Under confinement a turnover to the power-law  $\overline{\delta^2} \simeq (\Delta/T)^{1-\alpha}$  occurs [26, 27]. This second power-law regime is terminated when  $\Delta$  approaches the total measurement time  $T$ , causing a dip in  $\overline{\delta^2}$  back to the plateau of the ensemble average. The observed characteristic turnover behavior is intimately connected to CTRW ageing and ergodicity breaking [35, 36]. Corralled motion [37] could not explain the observed behavior  $\overline{\delta^2} \simeq \Delta$  turning over to  $\overline{\delta^2} \simeq \Delta^\beta$ .

The following features unanimously point toward CTRW subdiffusion as the stochastic mechanism for the granule motion at short times: (i) The time average  $\overline{\delta^2}$  initially scales linearly with  $\Delta$ , albeit the ensemble average shows subdiffusion of the type (1) in comparable time ranges. (ii) At longer times a turnover to the power-law  $\overline{\delta^2} \simeq \Delta^\beta$  occurs instead of the convergence to a plateau, which would necessarily occur for an ergodic process; the anomalous diffusion exponent  $\alpha \approx 0.80 \dots 0.85$  observed in the ensemble average is consistent with the exponents  $\beta \approx 0.15 \dots 0.20$  observed in Fig. 1 based on the relation  $\beta = 1 - \alpha$  [26, 27], as well as the slopes of the long time data (see below). (iii) The specific form of  $\overline{\delta^2}$  of the data nicely coincides with simulations results for a subdiffusive CTRW in an harmonic potential (Fig. 1). These observations prove that the granule motion in fact exhibits weak ergodicity breaking associated with subdiffusive CTRW processes. This is the central finding of this work.

We rule out the possibility that the initial CTRW simply turns over to much slower diffusion with  $\alpha \approx 0.15 \dots 0.20$ , as the overlapping video tracking data shows subdiffusion with  $\alpha \approx 0.8$  or slightly below. Also, CTRW or FBM trajectories with  $\alpha = 0.20$  would cause a quite extreme stalling or antipersistence, respectively, which is inconsistent with the recorded time series [Fig. 5 (SM)].

What results yield from complimentary criteria? (i) Evaluating  $\overline{\delta^2}(\Delta, T)$  as function of the total measurement time  $T$ , no ageing is observed [Fig. 6 (SM)], contrasting the scaling  $\overline{\delta^2}(T) \simeq T^{\alpha-1}$  predicted for CTRW subdiffusion with diverging mean waiting time  $\langle t \rangle$  [24–26]. (ii) Determining the distribution  $\phi(\xi)$  of the deviations of the relative time averaged mean squared displacement  $\xi = \overline{\delta^2}/\langle \overline{\delta^2} \rangle$  around the ensemble mean ( $\xi = 1$ ) we find the bell-shaped form of Fig. 2 with  $\phi(0) \approx 0$ . This form deviates from the predicted shape for CTRW subdiffusion with  $\langle t \rangle = \infty$  where  $\phi(0) \neq 0$  [24], see Fig. 2.

These seemingly conflicting observations can in fact be reconciled when we consider a power-law waiting time distribution with a cutoff effective at times  $t \gg \tau^*$ ,

$$\psi(t) = \frac{d}{dt} \left[ 1 - \frac{\tau^\alpha}{(\tau + t)^\alpha} \exp\left(-\frac{t}{\tau^*}\right) \right]. \quad (3)$$

Physically such cutoffs occur naturally in finite systems, corresponding to, e.g., a maximal well depth in a random

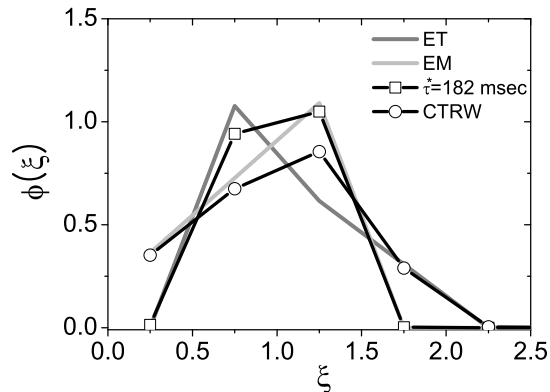


Figure 2: Distribution  $\phi(\xi)$  of the relative deviations  $\xi = \overline{\delta^2} / \langle \delta^2 \rangle$  of  $\delta^2$  obtained from averaging the data of Fig. 1 (Early Telophase, Early Mitosis). Simulations results are shown based on Eq. (3) with  $\tau^* = 182$  msec ( $\square$ ), and for a CTRW with  $\langle t \rangle = \infty$  ( $\circ$ ), with parameters  $\alpha = 0.85$ ,  $T = 3.0$  sec,  $\tau = 0.04545$  msec, and  $\Delta = 0.04545$  msec. See Fig. 7 (SM).

energy landscape. In free space Eq. (3) produces initial subdiffusion  $\langle \mathbf{r}^2(t) \rangle \simeq t^\alpha$ , turning over to  $\langle \mathbf{r}^2(t) \rangle \simeq t$  at  $t \gg \tau^*$ . As shown in Fig. 3 the cutoff-waiting time distribution (3) reproduces well the experimental behavior from Fig. 1. The scatter distribution  $\phi(\xi)$  [Figs. 2, 7 (SM)] shows excellent agreement, and the ageing plot [Fig. 6 (SM)] is consistent with the data. Here we chose the cutoff time  $\tau^* = 182$  msec, and  $\tau = 0.04545$  msec.

Collecting all results we conclude that at short times the granule motion is described by CTRW subdiffusion with truncated power-law waiting time distribution (3). While the cutoff ensures that the typical scaling of  $\overline{\delta^2}(\Delta, T)$  still exhibits the weak ergodicity breaking features, for appropriate choice of the cutoff time it is consistent with the absence of ageing effects, i.e.,  $\overline{\delta^2}(T) \simeq T^0$ , and the observed form for  $\phi(\xi)$ .

At longer times the motion of the lipid granules was recorded by video particle tracking. Fig. 4 shows the time averaged mean squared displacement. Initially the slope is around  $\alpha \approx 0.8$  or slightly below, consistent with the short time data. Several of the curves turn to a gentler slope at around 100 msec, some curves eventually switch to normal diffusion ( $\alpha = 1$ ) at 1 sec. Significant deviations are observed, which, for a living systems, is not surprising. Both the granule size and the materials properties of the cellular environment may change on these time scales (depolymerization/repolymerization of the cytoskeleton etc). As shown in Fig. 8 (SM) the distribution of  $\phi(\xi)$  is bell-shaped; no ageing is observed. Analysis of the moment ratios for both normal moments and the mean maximal excursion statistics (see Ref. [38] for details) are consistent with FBM for the range of  $\alpha \approx 0.80 \dots 0.85$  [Fig. 9 (SM)], as are typical antipersist-

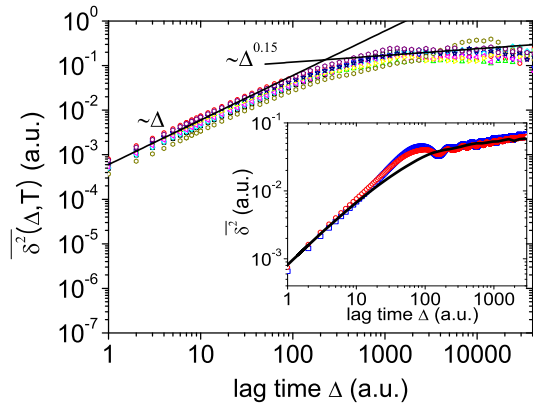


Figure 3: Time averaged mean squared displacement for a CTRW with waiting time cutoff (3) in an harmonic potential. Inset: Comparison of the average behavior of the simulated trajectories (—) and the average of the experimental data from Fig. 1 ( $\circ$ ,  $\square$ ). Parameters as in Fig. 2.

ent trajectories [Fig. 10 (SM)]. Moreover, the scaling exponents of the mean maximal excursion second moment are consistently above those of the corresponding regular second moments, as predicted for FBM [38]. The velocity autocorrelation of the data is consistent with both FBM and CTRW [Fig. 11 (SM)], and therefore is not conclusive. The p-variation method [31] was not conclusive.

Our analysis of extensive single particle tracking data of lipid granules in *S.pombe* cells demonstrates that at shorter times in the msec range the motion displays significant effects of weak ergodicity breaking both in the limit of free motion and in the presence of the restoring trap force. Concurrently no ageing occurs and the distribution of time averages  $\phi(\xi)$  is bell-shaped around  $\xi = 1$ . We showed that these features are consistent with a CTRW process with truncated power-law waiting time distribution. At longer times the motion is best described by subdiffusive FBM, although a conclusive statement in this time range is more difficult due to the fact that cellular processes appear to be superimposed on the motion. Physically, the CTRW-like motion may be associated with the interaction between granules and the semiflexible filaments of the cytoskeleton similar to the observations in Ref. [21]. While the behavior becomes more erratic in the long time data a turnover to a gentler slope is observed before a final increase to normal diffusion. This behavior may be connected to the viscoelastic properties of the complex cellular environment. The identification of FBM as stochastic mechanism is consistent with conclusions in Refs. [14, 16].

Lipid granules provide a natural, inert tracer to explore the diffusion properties inside living cells. Subdiffusion of large biopolymers in the cell supports the emerging, more local picture of cellular transport and regulation

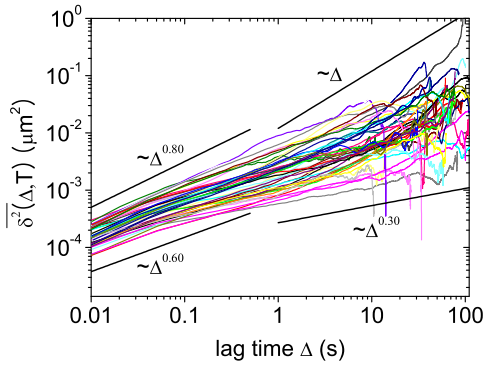


Figure 4: Time averaged mean squared displacement of granules in *S. pombe* (cells in interphase) from video tracking data (SM). An initial slope around  $\alpha \approx 0.8$  is found, turning over to a gentler slope. Several trajectories later exhibit  $\alpha \approx 1.0$ .

[39]. CTRW gives rise to a dynamic spatial localization [9, 35], while FBM provides a more compact spatial exploration and thus increases the local encounter probability [7]. Identifying these different subdiffusion mechanisms in cells can give new insights into *in vivo* molecular processes at different timescales.

This project was supported by the Deutsche Forschungsgemeinschaft (DFG), the CompInt Graduate School, and the Israeli Science Foundation.

---

[1] J. Mattsson et al., Nature **462**, 83 (2009); E. H. Zhou et al., Proc. Natl. Acad. Sci. **106**, 10632 (2009); A. Fierro et al., J. Stat. Mech. L04002 (2008).  
[2] A. Minton, J. Cell Sci. **119**, 2863 (2006); R. J. Ellis and A. P. Minton, Nature **425**, 27 (2003); S. B. Zimmerman and S. O. Trach, J. Mol. Biol. **222**, 599 (1991).  
[3] S. R. McGuffee and A. H. Elcock, PLoS Comput. Biol. **6**, e1000694 (2010).  
[4] R. Metzler and J. Klafter, Phys. Rep. **339**, 1 (2000); J. Phys. A **37**, R161 (2004).  
[5]  $\langle \cdot \rangle = \int \cdot P(\mathbf{r}, t) d\mathbf{r}$  denotes an ensemble average over the probability density  $P$  to find the particle at  $\mathbf{r}$  at time  $t$ .  
[6] C. Bräuchle, D. C. Lamb, and J. Michaelis, Editors, Single Particle Tracking and Single Molecule Energy Transfer (Wiley-VCH, Weinheim, 2010); M. J. Saxton and K. Jacobson, Ann. Rev. Biophys. Biomol. Struct. **26**, 373 (1997); S. Yamada, D. Wirtz, and S. C. Kuo, Biophys. J. **78**, 1736 (2000).  
[7] G. Guigas and M. Weiss, Biophys. J. **94**, 90 (2008).  
[8] I. Golding and E. C. Cox, Phys. Rev. Lett. **99**, 098102 (2006).  
[9] I. Bronstein et al., Phys. Rev. Lett. **103**, 018102 (2009).  
[10] G. Seisenberger et al., Science **294**, 1929 (2001).  
[11] A. Caspi, R. Granek, and M. Elbaum, Phys. Rev. Lett. **85**, 5655 (2000).  
[12] I. M. Tolić-Nørrelykke et al., Phys. Rev. Lett. **93**, 078102 (2004). The short time data presented here based on op-

tical tweezers tracking most likely correspond to the slow turnover region between the  $\overline{\delta^2} \simeq \Delta$  and  $\overline{\delta^2} \simeq \Delta^{1-\alpha}$  regimes, compare the discussion in Ref. [24].  
[13] C. Selhuber-Unkel, P. Yde, K. Berg-Sørensen, and L. B. Oddershede, Phys. Biol. **6**, 025015 (2009).  
[14] S. Weber et al, Phys. Rev. Lett. **104**, 238102 (2010).  
[15] J. Vercaemmen, G. Martens, and Y. Engelborghs, Springer Ser. Fluoresc. **4**, 323 (2007).  
[16] J. Szymanski and M. Weiss, Phys. Rev. Lett. **103**, 038102 (2009).  
[17] B. D. Hughes, Random walks and random environments. Vol. 1: Random Walks (Clarendon Press, Oxford, UK, 1995).  
[18] Also on fractal geometries subdiffusion prevails, see, e.g., [19] for a summary, or A. Klemm, R. Metzler, and R. Kimmich, Phys. Rev. E **65**, 021112 (2002) for an experiment. Here we do not consider this process.  
[19] S. Havlin and D. Ben-Avraham, Adv. Phys. **36**, 695 (1987).  
[20] C. Monthus and J.-P. Bouchaud, J. Phys. A **29**, 3847 (1996); S. Burov and E. Barkai, Phys. Rev. Lett. **98**, 250601 (2007).  
[21] I. Y. Wong et al., Phys. Rev. Lett. **92**, 178101 (2004).  
[22] A. N. Kolmogorov, Dokl. Acad. Sci. USSR **26**, 115 (1940); B. B. Mandelbrot and J. W. van Ness, SIAM Rev. **10**, 422 (1968).  
[23] W. T. Coffey, Yu. P. Kalmykov, and J. T. Waldron, The Langevin equation (World Scientific, Singapore, 2004).  
[24] Y. He, S. Burov, R. Metzler, and E. Barkai, Phys. Rev. Lett. **101**, 058101 (2008).  
[25] A. Lubelski, I. M. Sokolov, and J. Klafter, Phys. Rev. Lett. **100**, 250602 (2008).  
[26] S. Burov, R. Metzler, and E. Barkai, Proc. Natl. Acad. Sci. USA **107**, 13228 (2010). S. Burov, J.-H. Jeon, R. Metzler, and E. Barkai, Phys. Chem. Chem. Phys. (at press), E-print arXiv:1009.4846v2.  
[27] T. Neusius, I. M. Sokolov, and J. C. Smith, Phys. Rev. E **80**, 011109 (2009).  
[28] M. Weiss, M. Elsner, F. Kartberg, and T. Nilsson, Biophys. J. **87**, 3518 (2004).  
[29] D. Banks and C. Fradin, Biophys. J. **89**, 2960 (2005).  
[30] W. Pan et al., Phys. Rev. Lett. **102**, 058101 (2009).  
[31] M. Magdziarz, A. Weron, K. Burnecki, and J. Klafter, Phys. Rev. Lett. **103**, 180602 (2009).  
[32] At moderate distances from the trap center the potential felt by the trapped object is harmonic: A. C. Richardson, S. N. S. Reihani, and L. B. Oddershede, Optics Express **16**, 15709 (2008).  
[33] The voltage signal from the photodiode is directly proportional to the particle position relative to the trap center. Imprecise knowledge of the optical properties in the cell hampers a precise conversion to absolute length.  
[34] S. Burov and E. Barkai, Phys. Rev. Lett. **100**, 070601 (2008); Phys. Rev. E **78**, 031112 (2008).  
[35] E. Barkai and Y. C. Cheng, J. Chem. Phys. **118**, 6167 (2003).  
[36] J.-P. Bouchaud, J. Phys. (Paris) I, **2**, 1705 (1992); G. Bel and E. Barkai, Phys. Rev. Lett. **94**, 240602 (2005); A. Rebenshtok and E. Barkai, *ibid.* **99**, 210601 (2007); M. A. Lomholt, I. M. Zaid, and R. Metzler, *ibid.*, **98**, 200603 (2007); I. M. Zaid, M. A. Lomholt, and R. Metzler, Biophys. J. **97**, 710 (2009).  
[37] N. Destainville, A. Saulière, and L. Salomé, Biophys. J. **95**, 3117 (2008).

[38] V. Tejedor et al., *Biophys. J.* **98**, 1364 (2010).

[39] P. M. Llopis et al., *Nature* **466**, 77 (2010); G. Kolesov et

al., *Proc. Natl. Acad. Sci. USA* **104**, 13948 (2007).